AD-A094 735 AIR FORCE INST OF TECH WRIGHT-PATTERSON AFB OH SCHOO--ETC F/G 20/4
FLOW CHARACTERISTICS IN A CHANNEL FOLLOWING EXIT OF INCIDENT SH--ETC(U)
DEC 80 R H TATE

UNCLASSIFIED AFIT/GAE/AA/80D-20 NL

END
DATE FILMED
3 81
DTIC

23 JAN 1981

APPROVED FOR PUBLIC RELEASE AFR 190-17.

AFIT/GAE/AA/80D-20

Laurel A. Lampela

LAUREL A. LAMPELA, 2Lt, USAF
Deputy Director, Public Affairs

Air Force Institute of Technology (ATC)
Wright-Patterson AFB, OH 45433

FLOW CHARACTERISTICS IN A CHANNEL

FOLLOWING EXIT OF INCIDENT SHOCK WAVE

THESIS

AFIT/GAE/AA/80D-20 Ralph H. Tate, III
Capt USAF

Approved for public release; distribution unlimited

81 2 09 025

AFIT/GAE/AA/80D-20

# FLOW CHARACTERISTICS IN A CHANNEL FOLLOWING EXIT OF INCIDENT SHOCK WAVE

THESIS

Presented to the Faculty of the School of Engineering
of the Air Force Institute of Technology
Air Training Command
in Partial Fulfillment of the
Requirements for the Degree of
Master of Science

by

Ralph H. Tate, III
Capt USAF
Graduate Aeronautical Engineering

December 1980

Approved for public release; distribution unlimited

## Preface

I would like to thank my thesis advisor, Dr. William C. Elrod, for his encouragement, foresight and understanding during this research effort. I would also like to thank Dr. Harold E. Wright, Dr. James E. Hitchcock and Capt Aaron Dewispelare for serving on the thesis review committee and providing excellent assistance.

My appreciation also goes to Mr. Carl Shortt, Chief of the AFIT Model Fabrication Shop and to Mr. Jack Tiffany, Mr. Ron Ruley and Mr. Dave Murry for the very professional work they did in constructing the necessary models and test sections. I also wish to recognize Mr. George Gergal, Mr. H. LeRoy Cannon, and Mr. William Baker for their technical assistance.

Most of all, my appreciation and admiration goes to my wife, Carolyn, for her diligent and faithful support during times of discouragement as well as success.

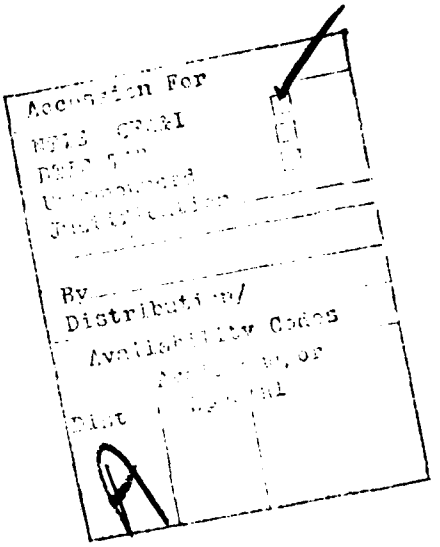

## Contents

## List of Symbols

$a_1$ ≡ speed of sound in shock tube driven section, ft/sec (m/sec)

$a_4$ ≡ speed of sound in shock tube driver section, ft/sec (m/sec)

C ≡ pressure gage correction factor

$d_1$ ≡ separation distance between sensors A and B, inches (meters)

$d_2$ ≡ separation distance between sensor B and shock location at end of computed time delay interval, inches (meters)

$f_1$ ≡ time delay computer fixed oscillator operating frequency, hertz

$f_2$ ≡ time delay computer variable oscillator operating frequency, hertz

Hg ≡ mercury

$h_{1,r}$ ≡ measured mercury manometer column height, inches ($N - m^{-2}$)

$M_s$ ≡ shock wave propagation Mach number(laboratory reference frame)

$M_{se}$ ≡ expected $M_s$ determined from theory (laboratory reference frame)

$M_{sm}$ ≡ calculated $M_s$ determined from data (laboratory reference frame)

$M_2$ ≡ flow Mach number behind shock wave (laboratory reference frame)

$P_a$ ≡ ambient pressure, inches of mercury ($N - m^{-2}$)

$P_g$ ≡ gage pressure, inches of mercury ($N - m^{-2}$)

$P_1$ ≡ shock tube driven section pressure, inches of mercury ($N - m^{-2}$)

$P_2$ ≡ shock tube pressure behind shock wave, inches of mercury ($N - m^{-2}$)

$P_{21}$ ≡ shock wave pressure ratio = $P_2 / P_1$

$P_{21e}$ ≡ expected $P_{21}$ determined from $M_{se}$

$P_{21m}$ ≡ calculated $P_{21}$ determined from $M_{sm}$

$P_4$ ≡ shock tube driver section pressure, inches of mercury ($N - m^{-2}$)

$P_{41}$ ≡ shock tube diaphragm pressure ratio = $P_4$ / $P_1$

$P_2'$ ≡ $P_2$ divided by initial $P_1$

$t$ ≡ time, seconds

$T_a$ ≡ ambient temperature, $^oR$

$U_s$ ≡ shock wave propagation velocity (laboratory reference frame), ft/sec (m/sec)

$U_2$ ≡ flow velocity behind shock wave (laboratory reference frame), ft/sec (m/sec)

$\gamma$ ≡ ratio of specific heat at constant pressure to specific heat at constant volume

$\gamma_1$ ≡ $\gamma$ for shock tube driven section

$\gamma_4$ ≡ $\gamma$ for shock tube driver section

$\Delta t_1$ ≡ time interval between shock arrival at sensor A and shock arrival at sensor B, microseconds

$\Delta t_2$ ≡ time interval between shock arrival at sensor B and signal output from time delay computer, microseconds

$P_6$ ≡ pressure behind incident shock wave in reduced area test section ($N - m^{-2}$)

$P_{61}$ ≡ shock wave pressure ratio in reduced area test section

$P_6'$ ≡ $P_6$ divided by initial $P_1$

$P_7$ ≡ pressure behind incident shock wave following exit from reduced area test section ($N - m^{-2}$)

## List of Figures

## List of Tables

## Abstract

Dynamic variations in pressure occurring within shock tube channels following the exit of an incident shock wave were investigated. Three channel sizes were investigated. The first size was 4 in by 8 in by 48 in (10.16 cm by 20.32 cm by 1.22m), the second size was 4 in by 1 in by 25 in (10.16 cm by 2.54 cm by 63.5 cm), and the third size was 1 in by 1 in by 44 in (2.54 cm by 2.54 cm by 1.12 m). For the first and second channels, the shock tube diaphragm pressure ratio, $P_{41}$, ranged from 6.0 to 20.0. The third channel was used over a $P_{41}$ range of 8.0 to 20.0 and also to determine the presence of transverse waves due to an area reduction in the shock tube. The first channel, having the same cross-sectional area as the shock tube, exhibited pressures which approximated simple shock tube theory results. The second and third channels exhibited complex pressure changes which consistently peaked at the same time after the shock wave passed the pressure sensors, independent of $P_{41}$.

# I. Introduction

Under conditions of very high entropy, as exhibited in chemical lasers, undesirable pressure waves can be generated which cause the efficiency of the system to be degraded. A discussion of the phenomenon of high entropy generated pressure waves will provide the foundation for this research effort.

A chemical laser utilizes a chemical reaction to achieve the necessary atomic or molecular population inversion necessary for excitation energy. In the case of a pulsed chemical laser, these reactions can be explosive in nature, generating a shock wave in the gas medium. As the shock wave propagates through the device, it may reflect from a fixed surface as a shock wave or from a free surface as an expansion fan. Depending upon the duration and intensity of these waves, as well as the internal configuration of the device, the pressure waves can generate a very complex pressure distribution which directly affects the power efficiency and pulse rate of the laser.

## Background

In an effort to understand the phenomenon of pressure waves in a confined cavity, shock tubes have historically been used as a shock wave generating source. A previous approach in attempting to eliminate both shock waves and expansion fans from propagating back into the shock tube was done by Jones and McCallum[7]. They successfully investigated using flat plates and grids as reflection eliminators, causing the negative and positive pressure waves to cancel each other prior to reentering the shock tube.

There may be conditions under which it is not possible to eliminate pressure waves, either with reflection eliminators or by other means. It then becomes necessary to consider the impact of this physical phenomenon on the system of interest.

## Objective

The objective of this research will be to obtain qualitative and quantitative measurements of pressure changes in a channel following the exit of an incident shock wave. This is to be accomplished by determining intensity and duration of shock waves and expansion fans for the defined conditions.

## Approach

Tests will be conducted in the Air Force Institute of Technology 4 in by 8 in by 20 ft (10.16 cm by 20.32 cm by 6.10 m) shock tube facility. Ambient temperature air will be used for both driven and driver gas. Shock tube performance estimates will be made using the basic relationships of Liepman and Roshko[8] and Shapiro[9].

The three test sections to be used in the experiment will be 1 in by 1 in, 4 in by 1 in, and 4 in by 8 in (2.54 cm by 2.54 cm, 10.16 cm by 2.54 cm, and 10.16 cm by 20.32 cm) in cross section. Surface mounted pressure transducers, located in each test section at known locations, will be used to obtain the data.

Before discussing the results of the investigation, it is necessary to first consider a few theoretical aspects of shock tubes and to discuss the unique features of the shock tube and instrumentation used for this research. Following these aspects, an analysis of the results obtained from the three test sections will be presented.

## II. Theoretical Considerations

To simplify the experimental conditions within the shock tube, the following assumptions are made: (1) 1-D flow shock wave prior to area change, 2-D flow afterward, (2) 1-D flow expansion waves, (3) air on both sides of diaphragm is stationary and at ambient temperature prior to diaphragm rupture, and (4) air is considered a perfect gas with $\gamma = 1.4$.

In order to increase the effective Mach number range of the shock tube above that obtained by simply pressurizing the driver section, two approaches are used: (1) the driven section is evacuated, increasing the diaphragm pressure ratio, $P_{41}$, and (2) the cross-sectional area of the shock tube is reduced through the test section region.

The operation of a simple shock tube can best be described with the aid of Fig 1. Prior to diaphragm rupture, the driver section is a region of high pressure ($P_4$) and the driven section is a region of low pressure ($P_1$). At the time of rupture, $t = 0$, a shock wave is initiated which moves through the region of low pressure while an expansion fan moves into the high pressure region. The contact surface between regions 2 and 3 represents the boundary between the gases that were initially on either side of the diaphragm. Regions 2 and 3 differ in temperature but have equal pressures and velocities.

After the shock wave exits the end of the tube, at $t = t_2$, an expansion fan begins to propagate back into the shock tube at sonic velocity, with respect to the gas medium into which it is moving. For the condition where the flow behind the shock wave is equal to or greater than the speed of sound, $M_2 \geq 1$, the expansion fan will not propagate

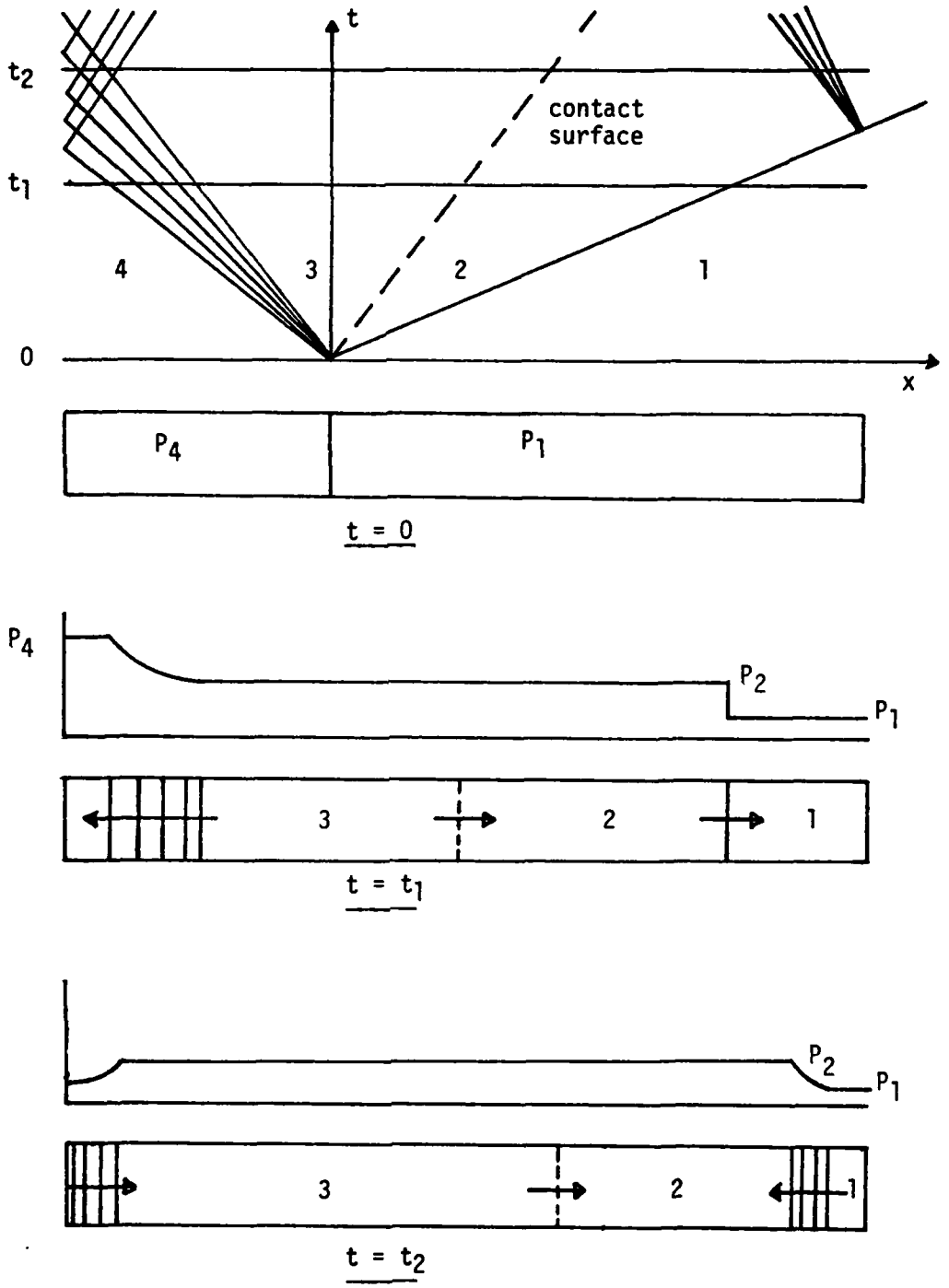


Fig 1. Simple Shock Tube Dynamic Processes

into the shock tube. With the condition that air at uniform temperature is used for both driver and driven gas, the sonic flow condition behind the shock wave is achieved when $M_s = 2.07$ [1].

The downstream pressure, $P_1$, remains constant after the exit of the shock wave from the shock tube if the shock wave expands into an infinite region. As the shock wave attempts to distribute its energy over its entire surface, the pressure difference across the shock diminishes as the shock surface becomes increasingly large.

For the shock tube with a reduced area test section, the dynamic processes behave in a more complex manner, as shown in Fig 2. As the incident shock wave moves into the reduced area test region, Fig 2b, a process occurs which is described by Tambra [10] as "coalescing" transverse waves. The area change causes the formation of these waves which move transverse to the initial flow, yet also remain attached to the incident shock wave as it moves down the test section. As the transverse waves move across the incident shock surface they tend to strengthen the incident shock but diminish in strength over distance. Along with the development of the transverse waves as a result of the area reduction, part of the incident shock wave is also reflected off the ramps and propagates back upstream.

Following the exit of the incident shock wave from the reduced area, Fig 2c, the shock wave will continue to move downstream as an expansion fan moves upstream into the reduced area region. If the expansion into the larger part of the test section does not dissipate the shock wave, pressure $P_7$ will remain higher than $P_1$. This condition reduces the strength of the expansion fan that moves back into the reduced area region. When the expansion fan reaches the upstream end of the reduced area test

section, it reflects off the "free surface" of the larger area as a series of compression waves, Fig 2d. These compression waves combine as they propagate through the test section to become a stronger single shock wave. Finally, as the incident shock wave leaves the end of the shock tube, another expansion fan moves upstream at a velocity determined by the $P_{71}$ ratio.

The theoretical method used to determine enhanced shock Mach numbers after an area change was to apply Whitham's rule [2,12]. This rule is an empirical relationship which assumes instantaneous Mach number changes following abrupt area changes. The method is elaborated in Appendix B. For the series of test runs, a computer program was written to calculate expected Mach numbers for the area reductions considered, given incremental $P_{21}$ ratios.

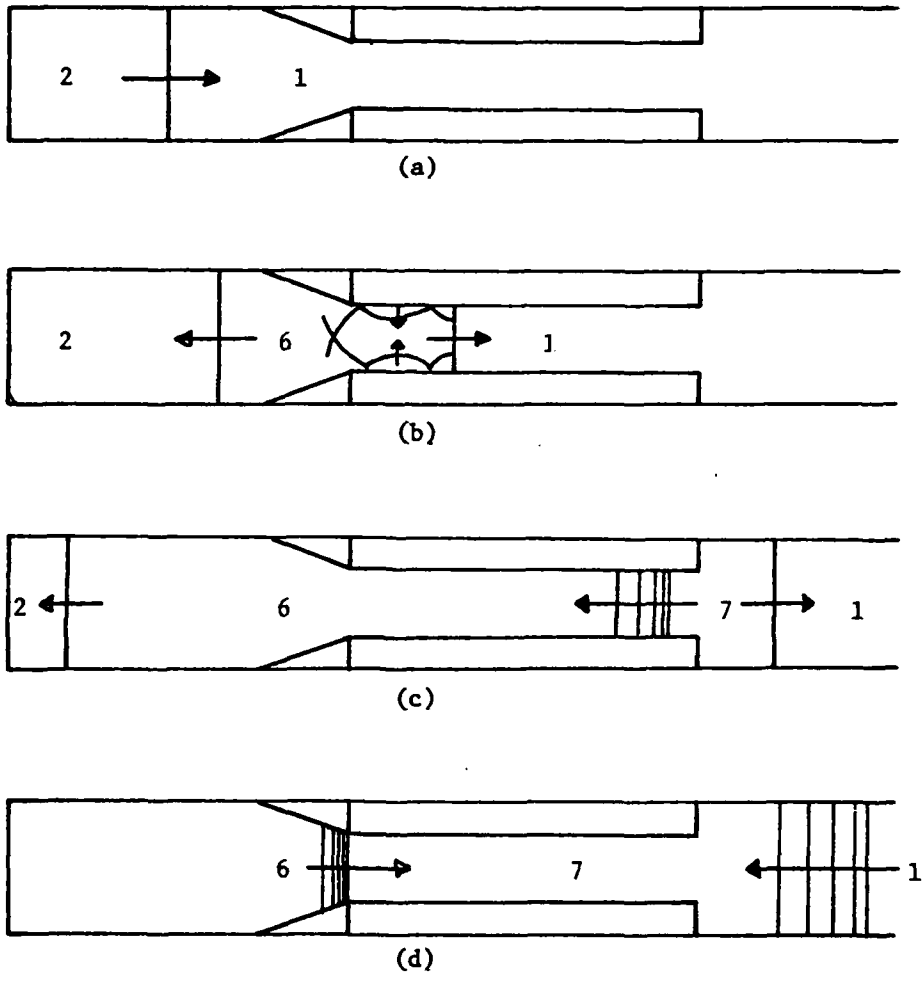


Fig 2. Reduced Area Shock Tube Dynamic Processes

## III. Apparatus

### Shock Tube System

The shock tube used in the research project was the Air Force Institute of Technology 4 in by 8 in by 20 ft (10.16 cm by 20.32 cm by 6.10 m) shock tube[3, 11]. The driver section is 4 ft (1.22 m) in length. This section is mounted on a sliding and traversing mechanism which permits access to both sections for cleaning. The driven section is 16 ft (4.88 m) in length, constructed of three straight 4 ft (1.22 m) sections and a changeable 4 ft (1.22 m) test section in which the internal dimensions can be altered. A shock dump tank which can be attached to the end of the shock tube will be described later.

Gas pressure in the driver section is monitored by a calibrated 0-200 in Hg (0 - 677.3 kN - $m^{-2}$) bourdon gage. Vacuum in the driven section is monitored by a 30 in Hg (101.59 kN - $m^{-2}$) manometer tube. Air was used as the driver and driven gas. The air supply was the filtered, dry compressed air from the building compressors. Maximum air supply pressure was approximately 228 in Hg (772.1 kN - $m^{-2}$) gage. Vacuum in the driven section was achieved by a Heraeus Model E 70 Vacuum pump. Maximum attainable vacuum with the dump tank attached was approximately 22 in Hg (74.5 kN - $m^{-2}$). Figure 3 is a diagram of the shock tube system.

The diaphragm used to maintain the pressure differential in the shock tube was Mylar, used in either single or multiple thicknesses. Previous reports indicated using no more than four sheets of Mylar at a time[3, 11]. In this investigation, no difficulties were experienced using 5 or 6 sheets of Mylar, $1x10^{-3}$ or $2x10^{-3}$ in ($2.54x10^{-5}$ or $5.08x10^{-5}$m) in

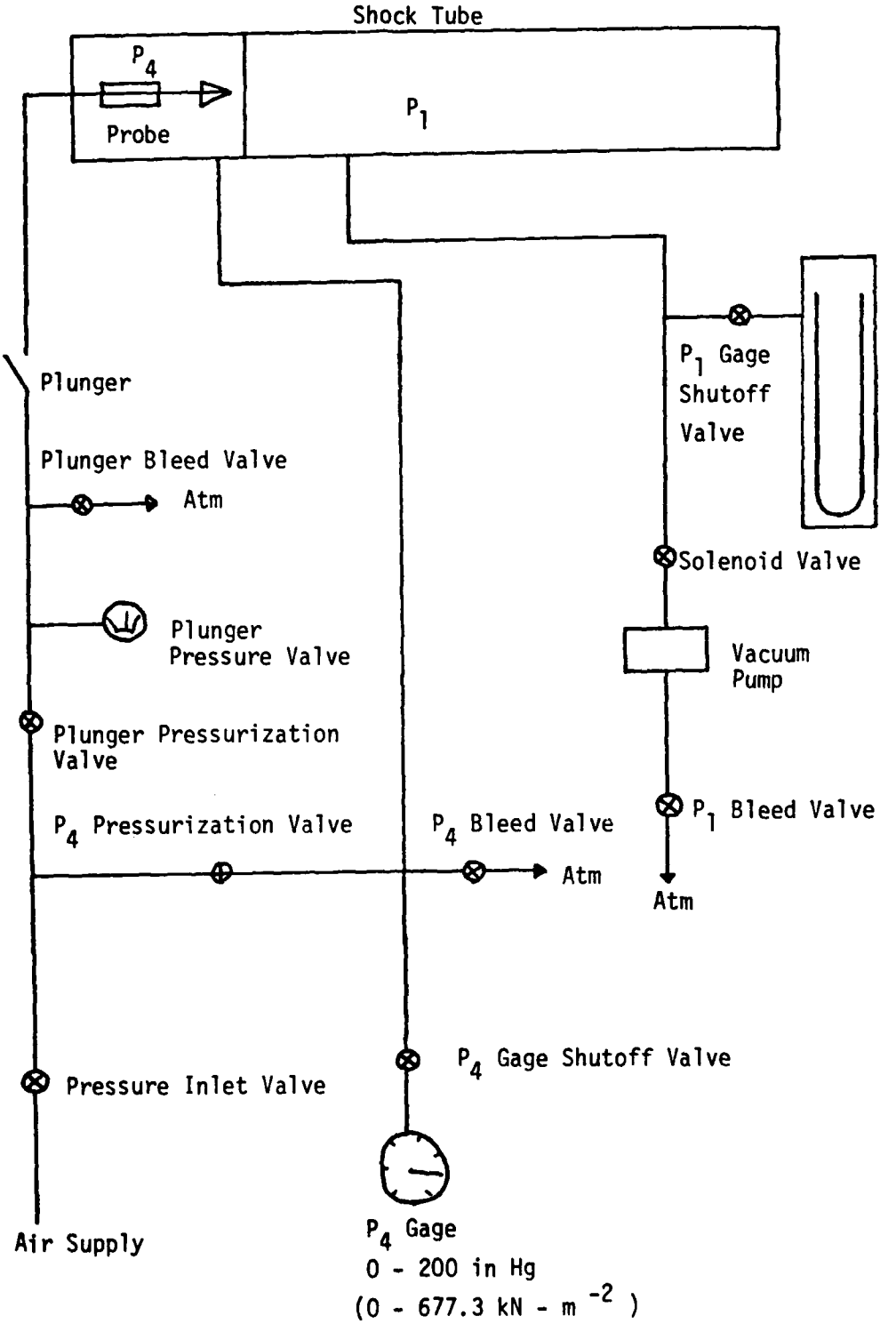


Fig 3. Shock Tube System

thickness.

Mylar is much more resistant to shattering upon rupture than other non-metallic materials and hence provides more consistent shock tube performance. Furthermore, it is necessary to establish the pressure differential as near the bursting strength of the diaphragm as possible to achieve the uniform shock velocity downstream in the shortest possible distance[4, 5]. The Mylar thickness required to maintain the pressure differential during this experiment was $4 \times 10^{-5}$ in/in Hg ($3 \times 10^{-7}$ m/kN - $m^{-2}$). Previous investigations have recommended greater thicknesses to maintain pressure differentials with this shock tube. The diaphragm was ruptured on command by a remotely controlled pyramidal probe.

Test Sections

Three 4 ft (1.22 m) test sections were used during the research. Significant dimensions for the test sections are shown in Fig 4. Test section 1 was used as a straight, unchanged section. Sections 2 and 3 were modified with pairs of rectangular wood blocks which provided a 1 in (2.54 cm) high open channel in the middle of the test sections. The straight taper ramps a and b, also in pairs, were positioned at the driver end of the appropriate test section. For test section 2, ramp a was used to reduce the height from 8 in (20.32 cm) to 1 in (2.54 cm). Test section 3 also used ramp a to reduce the height from 8 in (20.32 cm) to 1 in (2.54 cm) and used ramp b to reduce the width from 4 in (10.16 cm) to 1 in (2.54 cm).

Side View of Test Section

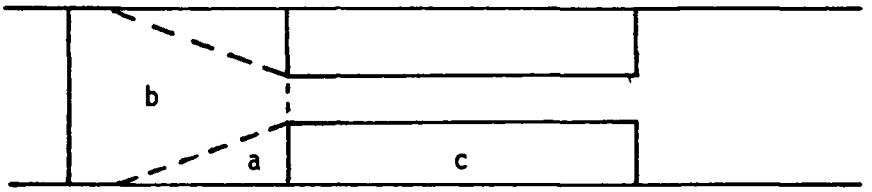


| | Test Section | | Ramp Length (in) | | Block Length (in) |
|---|---|---|---|---|---|
| | Width (in) | Height (in) | a | b | c |
| 1 | 4 | 8 | n/a | n/a | n/a |
| 2 | 4 | 1 | 16.25 | n/a | 25 |
| 3 | 1 | 1 | 16.25 | 24 | 44 |

Fig. 4. Straight Taper Ramps, Blocks and Test Sections

Upon initiation of the shock in a constant area shock tube with a closed end on the driven section, the shock propagates to the end of the driven section and is reflected back through the test region as a normal shock. In order to provide the condition of a shock wave exiting a confined channel and initiating the expansion fan process, the end of the shock tube was equipped with a shock dump tank. The tank is cylindrical in shape, 32 in (81.28 cm) in diameter and 6 ft (1.83 m) in length. The tank provides the additional benefits of allowing the driven section to be evacuated, dissipating the shock waves from the shock tube and delaying any shock reflections which might propagate into the test section. The dump tank was designed in a modular fashion to permit attachment to the end of all three test sections.

Electronic Instrumentation

The electronic instrumentation used for this research included pressure transducers, amplifiers, oscilloscopes, digital timers, a frequency oscillator, and a time delay computer. The electronics arrangement is presented diagrammatically in Fig 5. Sensors A and B, Endevco 8501-500 pressure transducers, were used to detect the incident shock speed and trigger the time delay computer. Sensors C and D, Endevco 8506-15 and 8506-50 pressure transducers, respectively, were used to measure the pressure fluctuations in the test sections caused by the shock waves and expansion fans. All transducers were surface mounted in the upper side of the test sections. For the three test configurations, the appropriate distances between transducers are given in Table 1.

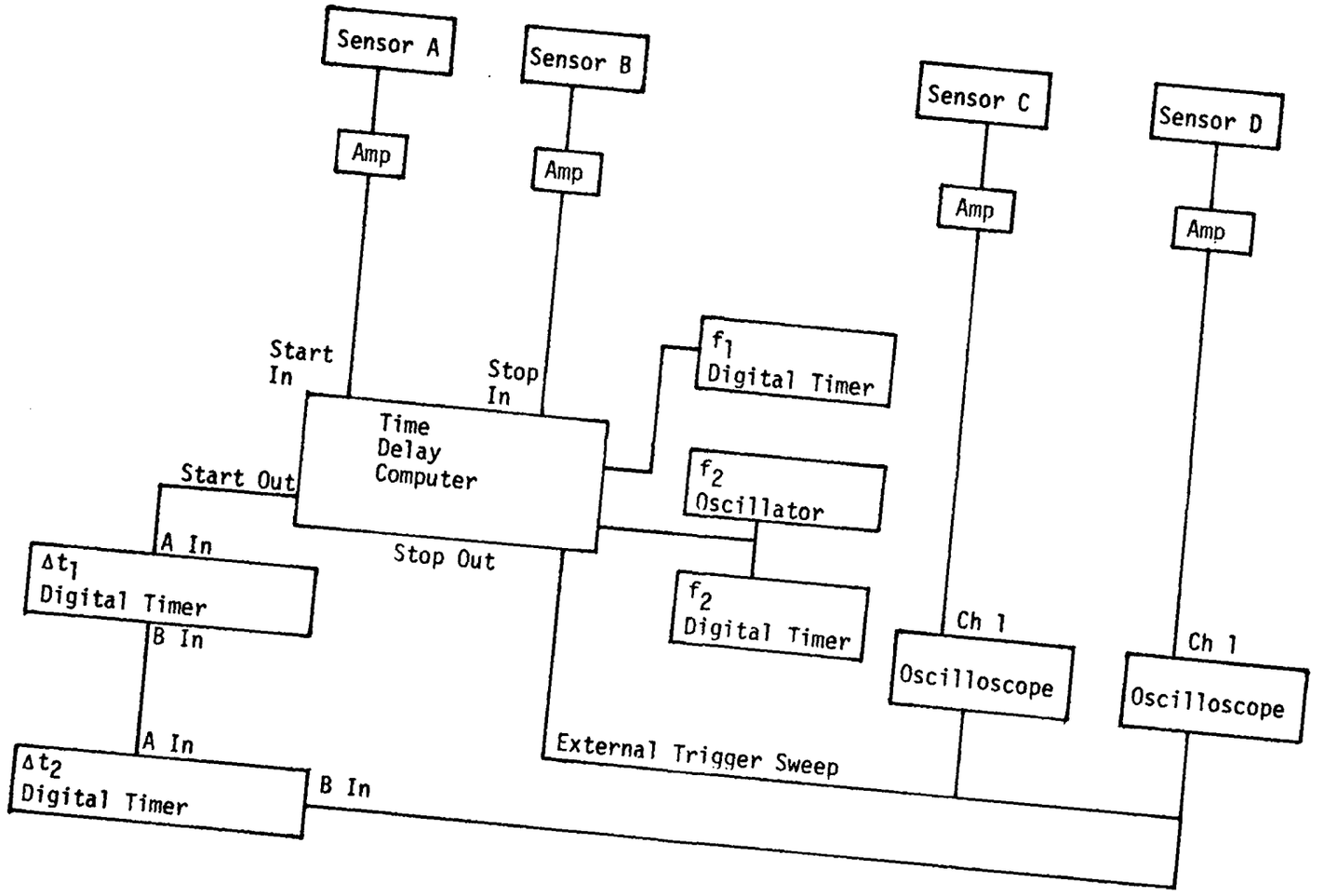


Fig 5. Electronic Arrangement

Table 1. Transducer Separation Distances

| Test Section | A to B (in) | B to C (in) | C to D (in) | D to end (in) |
|---|---|---|---|---|
| 1 | 12 | 43 | 6 | 3 |
| 2 | 2 | 4.125 | 2 | 4 |
| 3 | 2 | 4 | 2 | 4 |

The time delay computer developed by Weber[11] was used to trigger the sweep of the oscilloscopes. This was accomplished with the use of an internal counter used to count the number of pulses generated by a 10 Mhz ($f_1$) oscillator, starting from zero, as the incident shock wave traveled the distance $d_1$ from sensor A to sensor B.

The same number of pulses was then counted down to zero at the $f_2$ frequency rate as the shock moved a distance $d_2$. At that time an output signal was generated which externally triggered the oscilloscopes. For a constant shock speed, the frequency ratio $f_1/f_2$ is equal to the distance ratio $d_2/d_1$ and is independent of shock Mach number. The $f_2$ oscillator was therefore adjusted to initiate the sweep of the oscilloscopes with the shock at a position in the test section just prior to arrival at sensor C.

# IV. Results

## General

The emphasis of this research effort was to obtain pressure measurements, following the passage of an incident shock wave, in three different shock tube test sections, differing in cross-sectional area. In addition, test section 3 was used to verify the presence of "coalescing" tranverse waves following an area reduction in the shock tube, as described by Tambra[10].

In Tambra's work, he investigated the change in shock wave velocity due to the transverse waves following abrupt area changes over a $P_{41}$ pressure ratio of 4.0 to 7.0. He observed that as the shock travelled through the reduced area section, it varied in speed, usually increasing to a maximum velocity and then decreasing. The distance downstream of the area change at which the maximum velocity occurred changed very little with changes in $P_{41}$ but was dependent upon the area ratio of the reduced area to the initial area. As the area ratio decreased, the maximum speed location point moved toward the point of area change.

Toepler schlieren photography[6] was used to determine the presence of transverse waves immediately behind the incident shock in test section 3. Although the transverse waves were present at $P_{41}$ ratios similar to Tambra's study, they were weaker. This weakness may be attributable to the long distance downstream of the area change that the photographs were taken and to the tapered ramps. The long distance involved allowed the waves to diminish in strength whereas the ramps may have provided a different effect on the strength of the shock in the reduced area section than occurred for the abrupt area change investigated by Tambra.

Measured Mach numbers corresponded very well with results predicted by simple shock tube theory and Whitham's rule for the three test sections. For the determination of shock Mach number, $M_s$, over the $P_{41}$ range investigated, Whitham's rule, used for test sections 2 and 3, is almost as accurate as the theory of straight shock flow used for test section 1. Results for the three sections are given in Table 2. With the use of different thicknesses of Mylar sheets to produce the same total thickness required for a given $P_{41}$, $M_s$ varied less than 0.6% over the $P_{41}$ range investigated.

Figure 6 shows that the initial transient response of sensor C to the passage of the incident shock wave was not always the same with the same test conditions. One trace indicates a much faster and larger initial response to the shock wave than the other trace. However, the traces have the same value after approximately 50 μsec following the shock wave passage, indicating the same test section pressure.

For test sections 1 and 2, the $P_{41}$ ratios of 6.0 and 7.0 were the only runs in which the driven section was open to the atmosphere and the dump tank was not attached. The other tests were conducted with $P_1$ less than atmospheric pressure. In order to compare test results of the different $P_1$ pressures, transducer output signals were nondimensionalized by the initial driven pressure used for each run. This nondimensionalized test section pressure is $P_2'$ for test section 1 and $P_6'$ for test sections 2 and 3. The ratios $P_2'$ and $P_6'$ are equal to $P_{21}$ and $P_{61}$, respectively, for the condition when the incident shock wave passes the sensor.

Test Section 1

Figures 7 and 8 show the $P_2'$ responses recorded by sensors C and D in test section 1. As $P_{41}$ increases, the initial equilibrium $P_2'$ ratio

Table 2. Expected vs Measured Results for $M_s$, $P_{21}$ and $P_{61}$

| Test Section | $P_{41}$ | $P_1$(psia) | $M_{se}$ | $M_{sm}$ | % error | $P_{21e}$ | $P_{21m}$ | % error |
|---|---|---|---|---|---|---|---|---|
| 1 | 6.0 | 14.38 | 1.46 | 1.39 | 5.0 | 2.320 | 2.087 | 12 |
| | 7.0 | 14.21 | 1.50 | 1.43 | 4.9 | 2.458 | 2.219 | 11 |
| | 8.0 | 11.31 | 1.54 | 1.48 | 4.1 | 2.600 | 2.389 | 8.8 |
| | 10.0 | 9.35 | 1.61 | 1.54 | 4.5 | 2.857 | 2.600 | 9.9 |
| | 15.0 | 6.40 | 1.74 | 1.66 | 4.8 | 3.366 | 3.048 | 10 |
| | 20.0 | 5.41 | 1.83 | 1.76 | 4.0 | 3.740 | 3.447 | 8.5 |

| Test Section | $P_{41}$ | $P_1$(psia) | $M_{se}$ | $M_{sm}$ | % error | $P_{61e}$ | $P_{61m}$ | % error |
|---|---|---|---|---|---|---|---|---|
| 2 | 6.0 | 14.23 | 1.60 | 1.64 | -2.4 | 2.820 | 2.971 | -5.1 |
| | 7.0 | 14.23 | 1.66 | 1.68 | -1.2 | 3.048 | 3.126 | -2.5 |
| | 8.0 | 10.67 | 1.71 | 1.76 | -2.8 | 3.245 | 3.447 | -5.9 |
| | 10.0 | 9.35 | 1.79 | 1.84 | -2.7 | 3.571 | 3.783 | -5.6 |
| | 14.0 | 6.40 | 1.93 | 2.00 | -3.5 | 4.179 | 4.500 | -7.1 |
| | 20.0 | 4.43 | 2.07 | 2.21 | -6.3 | 4.832 | 5.531 | -12 |

| Test Section | $P_{41}$ | $P_1$(psia) | $M_{se}$ | $M_{sm}$ | % error | $P_{61e}$ | $P_{61m}$ | % error |
|---|---|---|---|---|---|---|---|---|
| 3 | 8.0 | 11.42 | 1.73 | 1.84 | -6.0 | 3.325 | 3.783 | -12 |
| | 10.0 | 9.45 | 1.82 | 1.97 | -7.6 | 3.698 | 4.361 | -15 |
| | 14.0 | 6.58 | 1.95 | 2.18 | -11 | 4.270 | 5.378 | -21 |
| | 20.0 | 5.60 | 2.09 | 2.43 | -14 | 4.929 | 6.722 | -27 |

also increases. However, in comparing with $P_{21m}$ from Table 2, $P_2'$ increases at a faster rate than $P_{21m}$. $P_2'$ also maintains a constant value for a longer period of time and does not exhibit as rapid a decrease as $P_{41}$ increases. The shock wave pressure ratio, $P_{21}$, and the Mach number of the flow behind the shock wave, $M_2$, increase with increasing $P_{41}$. These conditions slow the movement of the expansion fan into the test section and cause a delay in pressure decrease, with sensor C exhibiting the expansion fan effect later than sensor D. Table 3 compares the theoretical arrival times of the 1-D expansion fan phenomenon to the actual arrival times for the different $P_{41}$ ratios in test section 1. The times determined theoretically assume that when the constant velocity incident shock wave travels to the end of the reduced area section, the change in boundary conditions causes an expansion fan to immediately begin to propagate back into the reduced area section. The times include shock wave travel from the sensors to the end of the area reduction and the expansion fan travel back to the sensors. Due to the differences in velocities of the shock wave and the contact surface, and the length of the shock tube, the contact surface was determined not to arrive at the sensor locations until after the expansion fan process had occurred. The observation that the actual travel times are usually longer than the theoretical travel times indicates that the expansion fan probably does not start to propagate immediately after the shock wave exits the channel.

Rather than $P_2'$ exhibiting a continuous gradual decrease as a result of the expansion fan process, $P_2'$ decreases to an intermediate level before decreasing to its final value. This process is more apparent with sensor D. This suggests that the initial expansion fan that enters the test section establishes an equilibrium state which is subsequently followed by an additional expansion fan.

Table 3. Theoretical vs Experimental Propagation Times for Expansion Fan, Test Section 1

| $P_{41}$ | Actual Arrival Time (msec) | | Theoretical Arrival Time (msec) | |
|---|---|---|---|---|
| | C | D | C | D |
| 6.0 | 1700 | 600 | 1672 | 557 |
| 7.0 | 1700 | 600 | 1738 | 579 |
| 8.0 | 1900 | 760 | 1851 | 617 |
| 10.0 | 2200 | 750 | 2025 | 675 |
| 15.0 | 2700 | 1150 | 2543 | 848 |
| 20.0 | (obscured) | 1500 | 3249 | 1083 |

Test Section 2

Figures 9 and 10 are the $P_6'$ responses for sensors C and D in test section 2. These curves show the same trend as $P_2'$ in test section 1 for $P_6'$ to increase faster than $P_{61m}$ as $P_{41}$ increases. Immediately after the passage of the shock wave across the sensors, a decrease in $P_6'$ is followed by an increase and decrease. For both sensors C and D, this pressure spike appears to be related to $P_{41}$ because the $P_6'$ increase becomes larger as $P_{41}$ also increases. With sensor C, the increase also occurs at a progressively later time, moving from .45 msec to 1.16 msec after the incident shock wave, over the range of $P_{41}$. For sensor D, the occurrence of the $P_6'$ increase changes minimally.

For the lower values of $P_{41}$, the curves are similar to test section 1 except for the initial pressure disturbance. For $P_{41}$ of 6.0 and 7.0, the intermediate pressure plateau is present and is also present in the curves for $P_{41}$ of 8.0 and 10.0, but with the latter two it is followed

by a $P_6'$ increase instead of a decrease. For the range of $P_{41}$ from 8.0 to 20.0, the pressure rise continues to occur with its maximum value achieved at 6 msec following the passage of the shock wave. This pressure rise begins sooner after the passage of the shock wave as $P_{41}$ increases.

The $P_6'$ rise at 6 msec coincides with the time it would theoretically take for an expansion fan to propagate to the front of the reduced area section and return as a shock wave for $P_{41}$ ratios of 8.0 and 10.0, assuming a downstream pressure of $P_1$. This observation tends to support the idea that for these conditions, $P_7$ is approximately equal to $P_1$. The gradual change from pressure decrease to pressure increase over the range of $P_{41}$ is not understood, but for $P_{41}$ = 20, an expansion fan cannot enter the test section because $M_2>1$. Were the pressure rise a result of the expansion fan becoming a shock wave at the upstream end of the test section, the longer time required to propagate upstream would delay its occurrence and the wave would not be present at all for $P_{41}$ = 20. The very fact this is not what happens indicates the presence of a very complex system of pressure changes occurring in the shock tube with pressure increases becoming more dominant for increases in $P_{41}$. The complexity of pressure changes in the test section is apparently due to the reduction of cross-sectional area in the test section.

Test Section 3

Figures 11 and 12 are the $P_6'$ responses of sensors C and D in test section 3. From Table 2 there is a more significant difference between measured and expected values of $P_{61}$ in section 3 than in section 1 or 2. Despite this larger difference, the initial value of $P_6'$ in section 3

corresponds more closely to the measured value of $P_{61}$ over the range of $P_{41}$ than in section 1 or 2. As with section 2, a pressure disturbance occurs shortly after the passage of the incident shock wave. However, the time the disturbance occurs does not change as $P_{41}$ increases. For $P_{41}$ ratios of 8.0 and 10.0, the pressure curves are very similar to those of section 2. Even though $P_{61e}$ is larger in section 3 than section 2 due to the greater area reduction, the maximum value of $P_6'$ in section 3 is significantly less than in section 2. This suggests that as the distance changes downstream from the area change, the peak pressure achieved at that point in the test section will also change. The peak value for $P_6'$ still occurs at approximately 6 msec after shock wave passage.

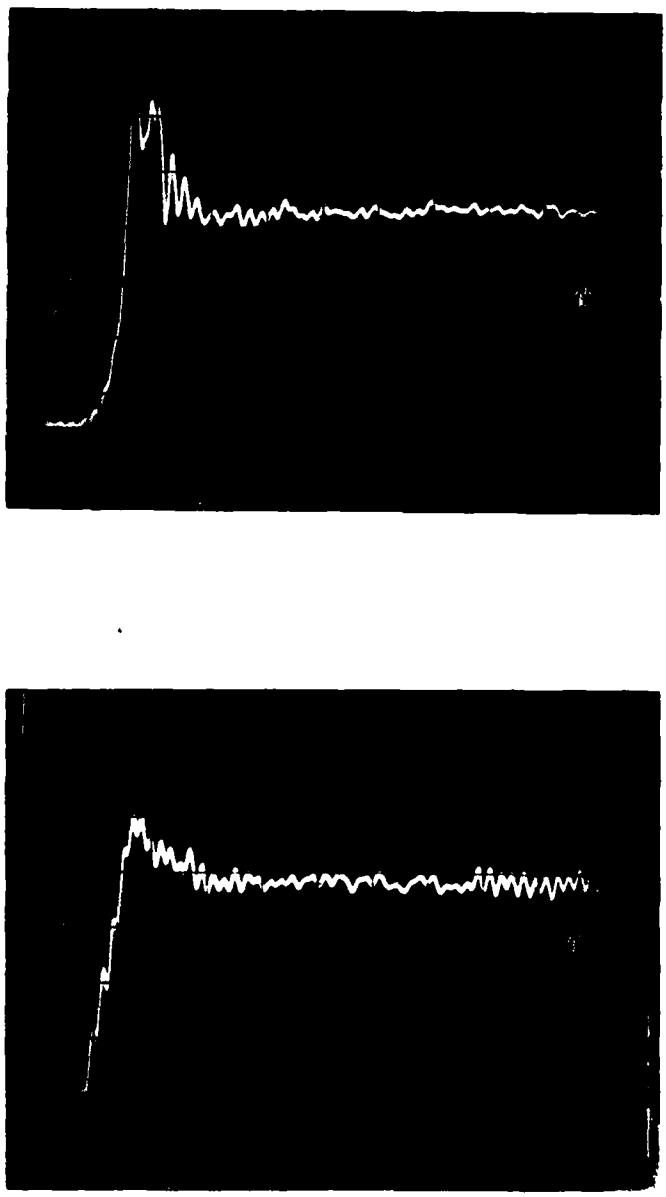

Fig. 6 Sensor C, Test Section 1 traces: $P_{41}$=6.0, 50 μsec/div

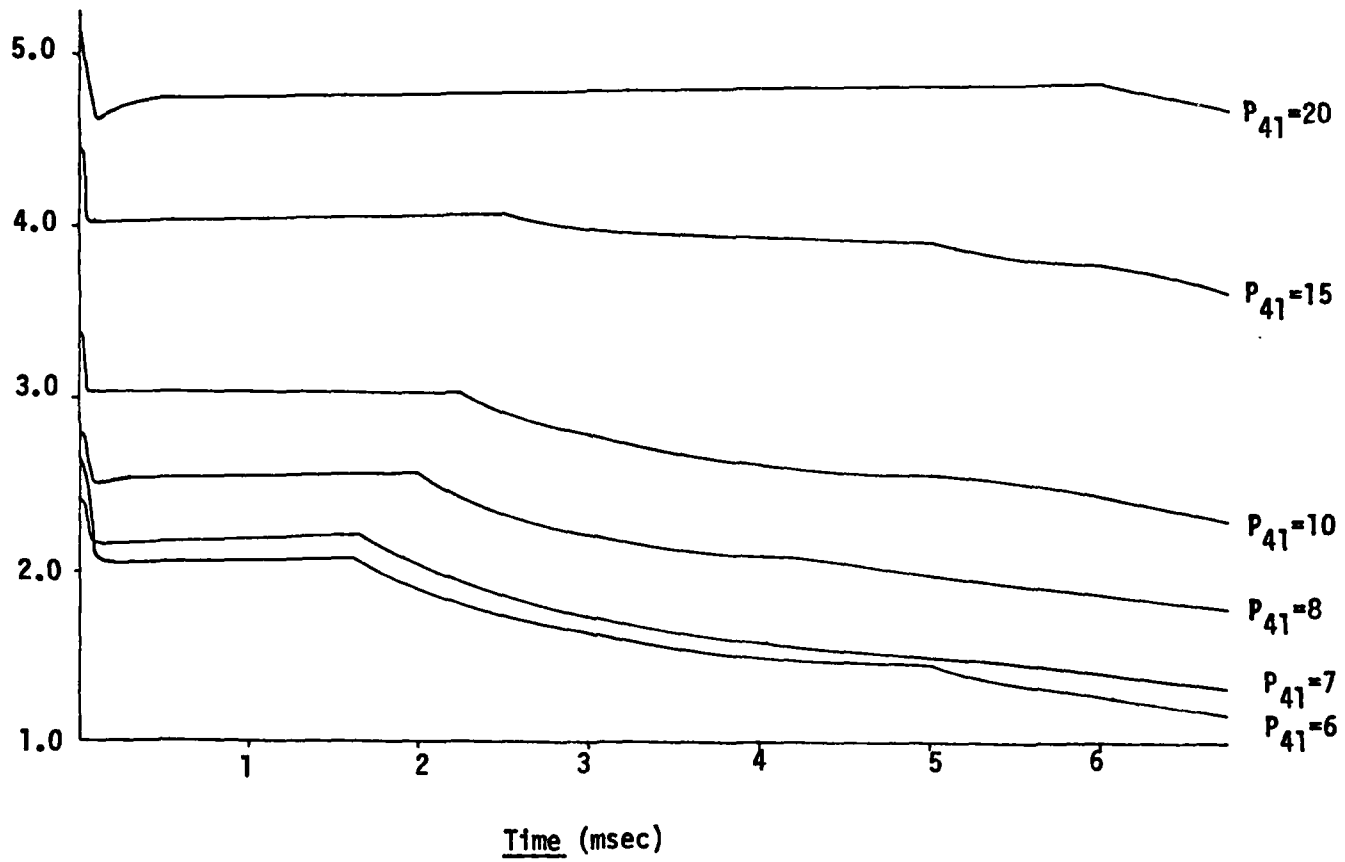


Fig. 7 $P_2'$ vs Time, Test Section 1, Sensor C

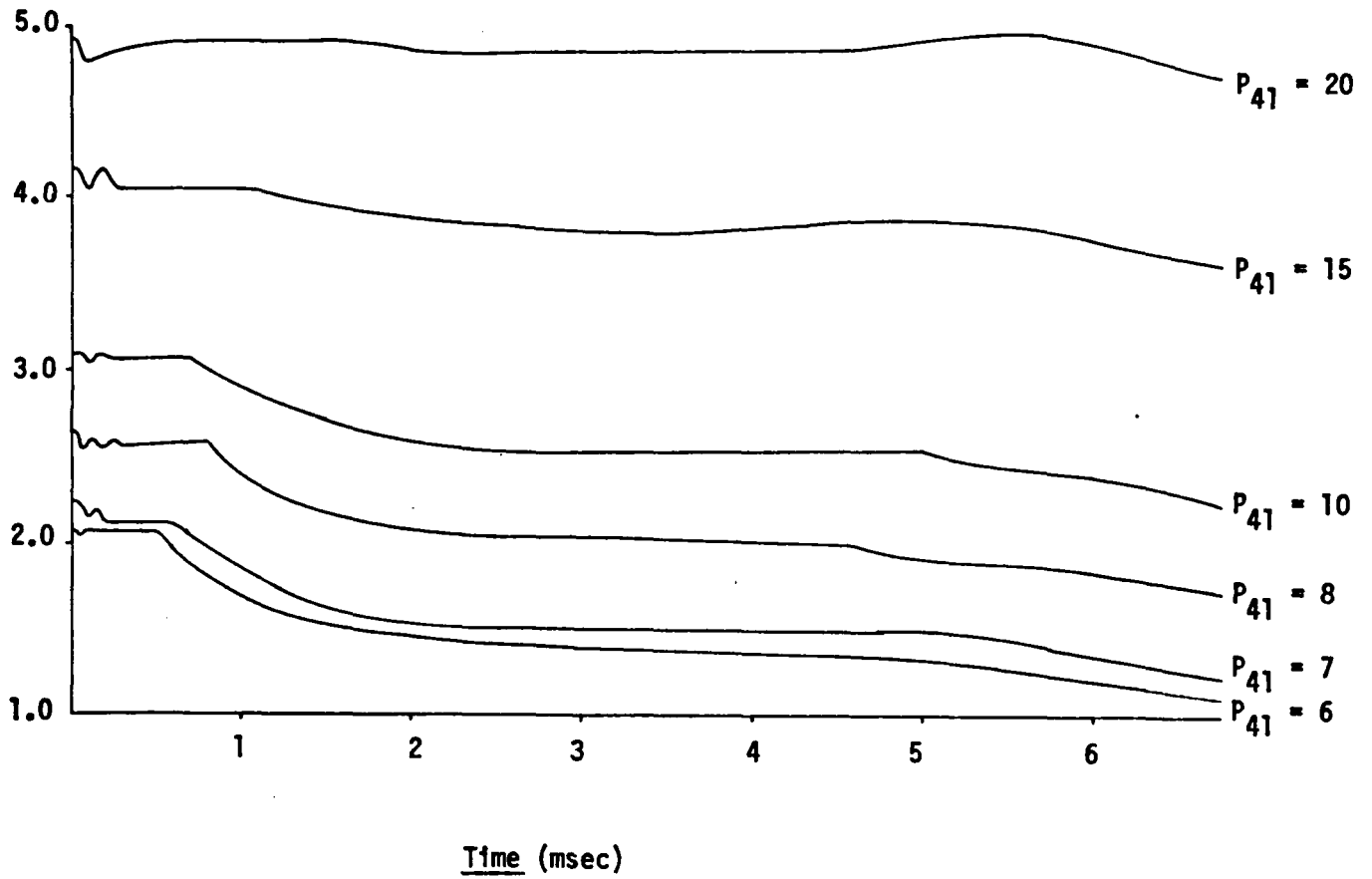


Fig. 8 $P_2'$ vs Time, Test Section 1, Sensor D

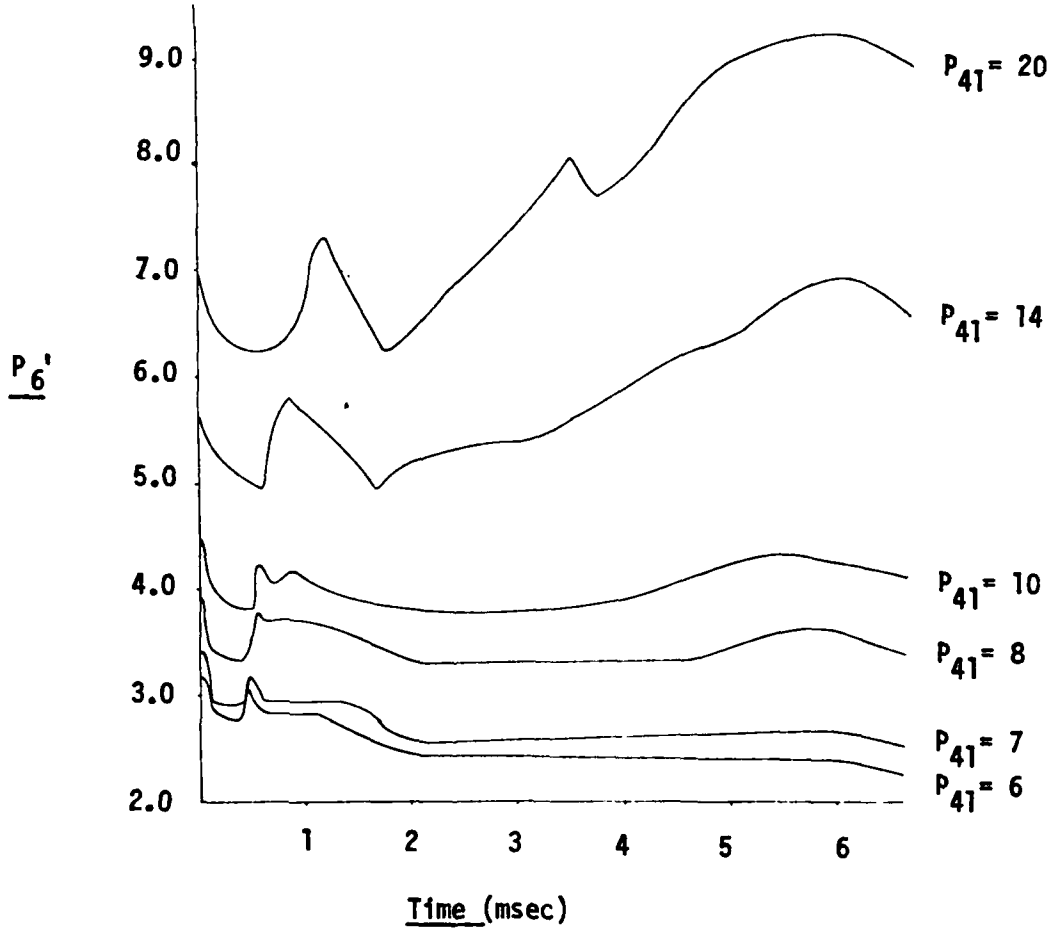


Fig. 9 $P_6'$ vs Time, Test Section 2, Sensor C

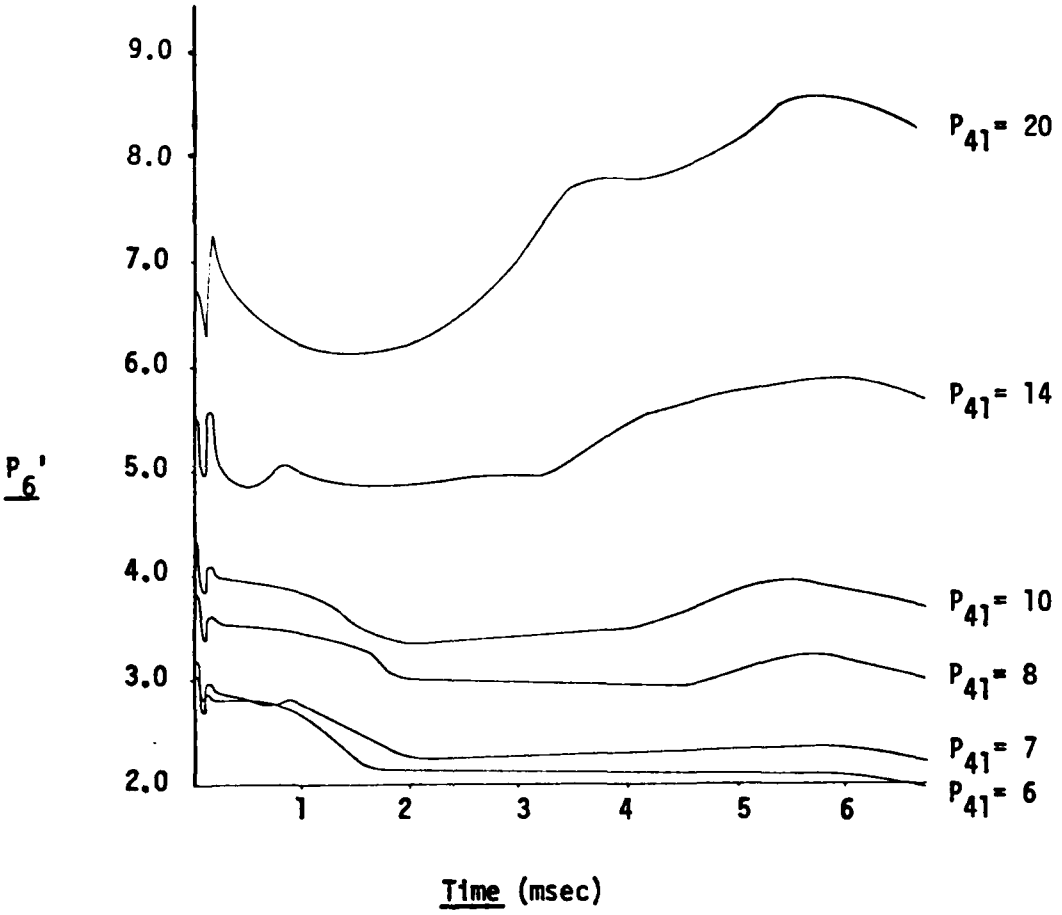


Fig. 10 $P_6'$ vs Time, Test Section 2, Sensor D

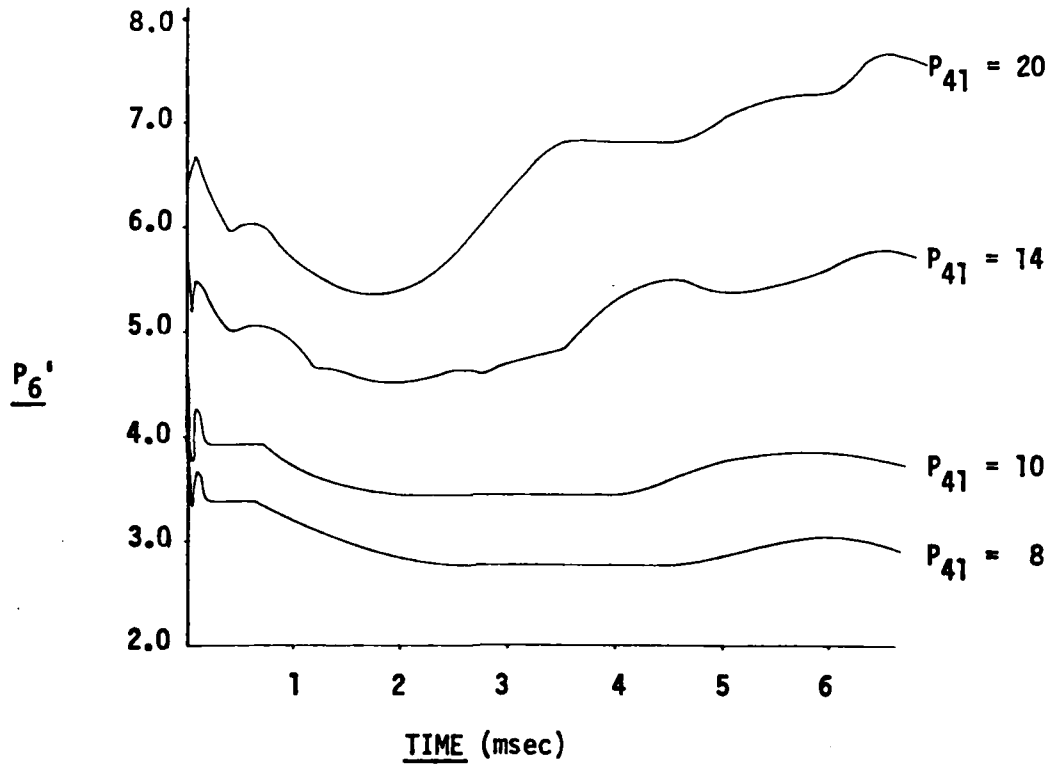


Fig. 11 $P_6'$ vs Time, Test Section 3, Sensor C

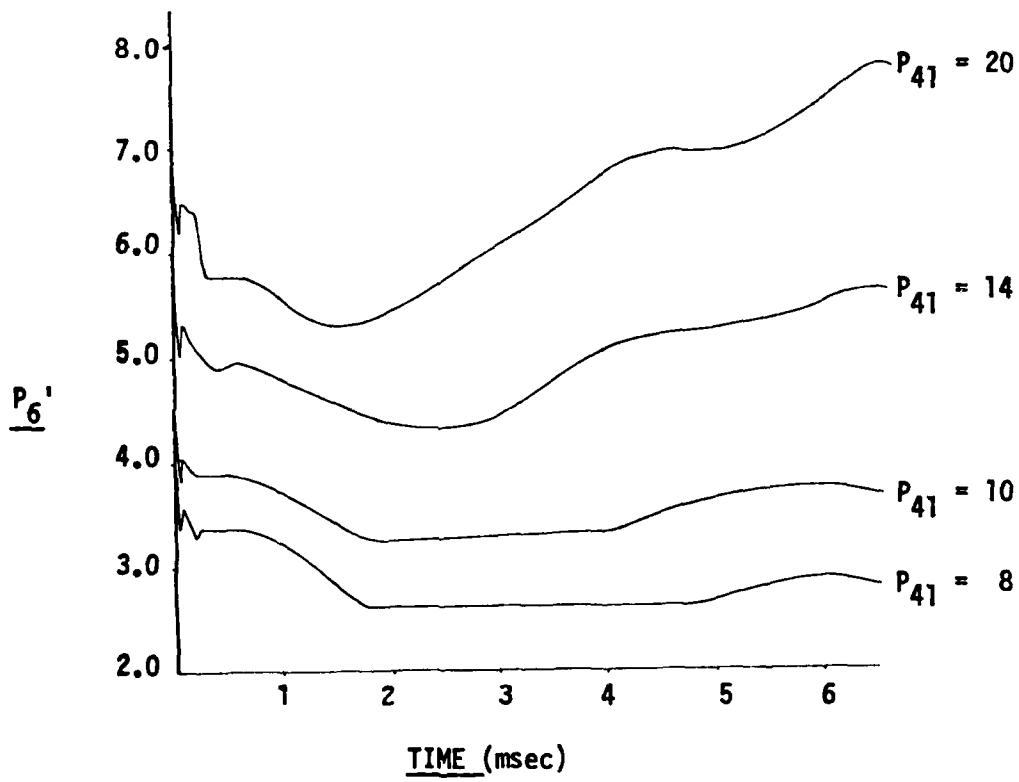


Fig. 12 $P_6'$ vs Time, Test Section 3, Sensor D

## V. Conclusions

The results of this investigation indicate pressure variations in a channel, after the exit of an incident shock wave, are significantly influenced by changes in length and cross-sectional area. In a constant area shock tube, for a $P_{41}$ range of 6.0 to 20.0, the expansion fan process is the dominant pressure influence. In a shock tube with an area change, the pressure variation becomes a much more complex sequence of pressure changes following the incident shock exit.

In test section 1, the expansion fan process following the exit of the incident shock wave does not appear to be a continuous process, but one that occurs in several quasi-continuous increments. In addition, the initial $P_{21}$ ratio, as determined from $P_2'$, becomes increasingly larger than expected as $P_{41}$ increases.

In test sections 2 and 3, the expansion fan process is observable at the lower $P_{41}$ ratios investigated and behaves in a similar manner to the process in test section 1. As $P_{41}$ increases, large pressure increases become the dominant pressure variation within the test section. The pressure increases consistently occur at approximately the same time after the passage of the incident shock wave regardless of $P_{41}$. The intensity of the pressure increases is a function of length and cross-sectional area of the test sections. In test section 2, as in test section 1, the initial $P_{61}$ ratio, determined from $P_6'$, becomes increasingly larger than expected as $P_{41}$ increases. Due to the complex nature of the flow behind the incident shock wave in a shock tube with a reduced area test section, additional investigation is necessary to explain these occurrences.

## VI. Recommendations

There are several recommendations that can be proposed for additional research in this area of study:

1. Use 4 in (10.16 cm) wide test section for optical investigation of transverse wave phenomenon in conjunction with pressure sensors positioned along the entire length of the test section. This would permit determination if the pressure fluctuations may be correlated with the transverse wave phenomenon.

2. Investigate study of pressure fluctuations in reduced area sections which extend through the entire test section. This study would eliminate any effects caused by a change in boundary conditions within the test section prior to the exit of the shock wave from the end of the test section.

3. Investigate and compare results in similar test sections with a shock wave generated by a chemical reaction or by electric discharge.

## Bibliography


1. Ames Research Staff, Ames Aeronautical Laboratory, Moffett Field, CA. Equations, Tables and Charts for Compressible Flow. NACA Report 1135, 1953.

2. Dvir, M., et al. "Effects of Cross-Sectional Area Change on the Speed of a Shock Wave". SR-2. The Hebrew University, Jerusalem, Israel, April 1966.

3. Egan, Douglas S., Jr., 1Lt, USAF, and Robert A. Foster, 1Lt, USAF. "Gas Dynamics Research with the Air Force Institute of Technology Shock Tube". Master's Thesis. Air Force Institute of Technology, Wright-Patterson AFB, OH., August 1956.

4. Glass, I. I. Shock Tubes: Theory and Performance of Simple Shock Tubes. UTIA Review No. 12, Part I. Institute of Aerophysics, University of Toronto, May 1958.

5. Hall, J. Gordon. Shock Tubes: Production of Strong Shock Waves, Shock Tube Applications, Design, and Instrumentation. UTIA Review No. 12, Part 2. Institute of Aerophysics, University of Toronto, May 1958.

6. Holder, D. W. and R. J. North. Optical Methods for Examining the Flow in High-Speed Wind Tunnels, Part I: Schlieren Methods. AGARDOGRAPH 23. North Atlantic Treaty Organization, Advisory Group for Aeronautical Research and Development, Paris, France, November 1956.

7. Jones, W. A. and F. L. McCallum. "Removal of the Reflected Pressure Pulses from the end of a Shock Tube". DRES Suffield Technical Note No. 257, April 1970.

8. Leipman, H. W. and A. Roshko. Elements of Gasdynamics. New York: John Wiley and Sons, Inc. 1957.

9. Shapiro, Ascher H. The Dynamics and Thermodynamics of Compressible Fluid Flow, Volume I, New York: The Ronald Press Company, 1953.

10. Tambra, Mohammed Latif, Sq Ldr. PAF. "The Interaction of a Moving Shock with an Abrupt Area Reduction in a Shock Tube". Master's Thesis. Air Force Institute of Technology, Wright-Patterson AFB, OH., 1970.

11. Weber, Paul A., Capt., USAF. "Shock Induced Starting of Gasdynamic Laser Nozzles". Master's Thesis. Air Force Institute of Technology, Wright-Patterson AFB, OH., December 1979.

12. Whitham, G. B. "On the Propagation of Shock Waves Through Regions of Non-Uniform Area of Flow," Journal of Fluid Mechanics, 4:337 (1958).

## Appendix A

### Experimental Procedure

Initial configuration:

- $P_1$ and $P_4$ gage shutoff valves - open
- $P_4$ pressurization and $P_4$ bleed valves - closed
- Plunger and plunger bleed valves - closed
- All nonessential valves - closed

1. Clean shock tube and install appropriate thicknesses of diaphragm material.
2. Zero all digital timers and oscilloscopes and set sweep trigger on oscilloscopes.
3. Adjust frequency $f_2$ for desired shock location.
4. Open vacuum solenoid valve, start vacuum pump and open plunger valve.
5. Open $P_4$ pressurization valve.
6. When desired diaphragm pressure ratio is reached, close vacuum solenoid valve.
7. Close $P_4$ and $P_1$ gage shutoff valves and remotely rupture diaphragm.
8. Shut off vacuum pump, close plunger valve, open plunger bleed valve and $P_1$ gage shutoff valve and open $P_4$ pressurization valve more to allow internal pressure to reach atmospheric level.
9. Record digital timers $\Delta t_1$ and $\Delta t_2$ . Photograph oscilloscope traces.
10. Mark photographs to correspond with numbered test run.
11. When $P_1$ gage pressure reaches atmospheric pressure close $P_4$ pressurization valve and plunger bleed valve and open $P_4$ gage shutoff valve.
12. Open shock tube, reset plunger probe and clean out shock tube debris as necessary.

## Appendix B

### Instrumentation Configuration

Wavetek Model 186 5 Mhz Phase Lock Sweep Generator

Frequency: adjustable

Freq Multiplier Switch: x 1M, x 10K

Symmetry: Normal

Gen Mode: Continuous

Signal Output: Pulse Out (TTL)

Computer Measurements Company Model 726C Universal Counter-Timer

(Configuration for $f_1$ and $f_2$ )

Function: Freq A

Freq - Time - N: $10^4$

Input A: DC

Gate: Auto

Slope: ( - )

Hewlett-Packard Model 5325B Universal Counter

($\Delta t_1$ configuration)

Time Base: .1 μsec

Selection: T.I. A to B

Channel A: Atten: x 10

AC

Slope: ( - )

Channel B: Atten: x 10

AC

Slope: ( + )

($\Delta t_2$ configuration)

Time Base: .1 μsec

Selection: T. I. A to B

Channel A: Atten: x 10

AC

Slope: ( - )

Channel B: Atten: x 10

DC

Slope: ( - )

Tektronix Model 434 Storage Oscilloscopes

Mode: single

Trigger Source: external

Slope: ( + )

Level: ( + )

Ext Attenuation: 1:1

LF Rej: off

HF Rej: off

Coupling: DC

Electro Instruments Model A20B-1 Amplifier Specifications

Full Scale Voltage: ± 10 vdc or peak AC to 20 Khz

Linearity: DC: ± .01% max (100 ohm min load)

AC: DC slew shift not more than ± .01% of peak AC up to 1 Khz

Freq Response: ± 1% DC to 2 Khz, 1 db to 20 Khz, 3 db to 50 Khz

## APPENDIX C

## Data Reduction

### Whitham's Rule

$$\frac{\delta A}{A} = \frac{-2M}{(M^2 - 1)k(M)} \delta M$$

where $$K(M) = 2\{(1 + \frac{2}{\mu + 1} \frac{1 + \mu^2}{\mu}) (2\mu + 1 + M^{-2})\}^{-1}$$

and $$\mu^2 = \frac{(\gamma - 1)M^2 + 2}{2\gamma M^2 - (\gamma - 1)}$$

For $A_1$ = 32 sq in (206.5 sq cm), $A_2$ = 4 sq in (25.8 sq cm) and $M_s$ = 1.60:

$$\mu^2 = .44681$$

$$K(M) = .43398$$

$$\text{and } \frac{\delta A}{A} = \frac{A_1 - A_2}{A_1} = .875$$

Therefore $\delta M = .185$

and $M_s = 1.60 + .185 = 1.785$ following the area change.

Pressure Ratio Calculation

$$P_4 = P_g \times C + P_a = P_g \times 1.002 + P_a$$

$$P_1 = P_a - h_{1,r}$$

For $P_a$ = 29.02 in Hg (98.277 kN - $m^{-2}$),
$P_g$ = 145 in Hg (491.047 kN - $m^{-2}$), and
$h_{1,r}$ = 7.3 in Hg (24.722 kN - $m^{-2}$):

$$P_4 = 145 \times 1.002 + 29.02 = 174.3 \text{ in Hg } (590.272 \text{ kN} - m^{-2})$$

$$P_1 = 29.02 - 7.3 = 21.72 \text{ in Hg } (73.555 \text{ kN} - m^{-2})$$

$$P_{41} = \frac{174.3}{21.72} = 8.0$$

Fundamental Pressure Ratio

$$P_{41} = P_{21} \left\{1 - \frac{(\gamma_4 - 1)(a_1/a_4)(P_{21} - 1)}{\sqrt{2\gamma_1}\sqrt{2\gamma_1 + (\gamma_1 + 1)(P_{21} - 1)}}\right\}^{-2\gamma_4/(\gamma_4 - 1)}$$

Shock Mach Number ($M_s$)

$$M_s = \left\{\frac{\gamma_1 - 1}{2\gamma_1} + \frac{\gamma_1 + 1}{2\gamma_1} P_{21}\right\}^{.5}$$

Mach Number of flow behind shock ($M_2$)

$$M_2 = \frac{1}{\gamma_1}(P_{21} - 1)\left\{P_{21}\left(\frac{\gamma_1 + 1}{2\gamma_1} + \frac{\gamma_1 - 1}{2\gamma_1} P_{21}\right)\right\}^{-.5}$$

Normalized $P_2$ ($P_2'$)

$P_2 = P_a + P_g$ where $P_g$ is determined by vertical displacements of oscilloscope traces from the 0 dc line.

$P_2' = P_2/P_1$

For $P_a$ = 29.02 in Hg = 14.26 psia (98.277 kN - $m^{-2}$) and

$P_g$ = 5 div x 100 mv/div ÷ 25.45 mv/psi

= 19.65 psig (135.42 kN - $m^{-2}$)

$P_1$ = 9.02 in Hg = 4.43 psia (30.547 kN - $m^{-2}$)

$$P_2' = \frac{14.26 + 19.65}{4.43} = 7.65$$

## Vita

Ralph Hamilton Tate III was born on 30 June 1952 in Syracuse, New York. He is the son of Ralph H. Tate Jr. and Ruth E. Tate. After graduating in 1970 from Bellevue Senior High School, Bellevue, Nebraska, he attended the U.S. Air Force Academy. He graduated from the Air Force Academy in 1974 with a B.S. in Aeronautical Engineering. Following graduation, he was assigned to the 90th Strategic Missile Wing, F.E. Warren AFB, Wyoming, as a missile launch officer. He served in that capacity until his reassignment to the Air Force Institute of Technology in June 1979. Captain Tate is married to the former Carolyn Kriesel of Gladstone, Nebraska.

UNCLASSIFIED

SECURITY CLASSIFICATION OF THIS PAGE *(When Data Entered)*

| REPORT DOCUMENTATION PAGE | READ INSTRUCTIONS BEFORE COMPLETING FORM |
|---|---|
| 1. REPORT NUMBER: AFIT/GAE/AA/80-20 — 2. GOVT ACCESSION NO.: AD-094735 | 3. RECIPIENT'S CATALOG NUMBER |
| 4. TITLE *(and Subtitle)*: FLOW CHARACTERISTICS IN A CHANNEL FOLLOWING EXIT OF INCIDENT SHOCK WAVE | 5. TYPE OF REPORT & PERIOD COVERED: Master's Thesis |
| | 6. PERFORMING ORG. REPORT NUMBER |
| 7. AUTHOR(s): Ralph H. Tate III, Captain USAF | 8. CONTRACT OR GRANT NUMBER(s) |
| 9. PERFORMING ORGANIZATION NAME AND ADDRESS: Air Force Institute of Technology (AFIT/EN), Wright-Patterson AFB OH 45433 | 10. PROGRAM ELEMENT, PROJECT, TASK AREA & WORK UNIT NUMBERS |
| 11. CONTROLLING OFFICE NAME AND ADDRESS: Air Force Institute of Technology (AFIT/EN), Wright-Patterson AFB OH 45433 | 12. REPORT DATE: December 1980 |
| | 13. NUMBER OF PAGES: 47 |
| 14. MONITORING AGENCY NAME & ADDRESS *(if different from Controlling Office)* | 15. SECURITY CLASS. *(of this report)*: UNCLASSIFIED |
| | 15a. DECLASSIFICATION/DOWNGRADING SCHEDULE |

16. DISTRIBUTION STATEMENT *(of this Report)*

Approved for public release; distribution unlimited.

17. DISTRIBUTION STATEMENT *(of the abstract entered in Block 20, if different from Report)*

18. SUPPLEMENTARY NOTES

Approved for public release; IAW AFR 190-17

FREDRIC C. LYNCH, Major, USAF
Director of Public Affairs
30 DEC 1980

19. KEY WORDS *(Continue on reverse side if necessary and identify by block number)*

Shock Tube
Shock Propagation
Shock Tube Instrumentation
Time Delay Computer
Whitham's Rule
(P sub 41)

20. ABSTRACT *(Continue on reverse side if necessary and identify by block number)*

Dynamic variations in pressure occurring within shock tube channels following the exit of an incident shock wave were investigated. Three channel sizes were investigated. The first size was 4 in by 8 in by 48 in (10.16 cm by 20.32 cm by 1.22 m), the second size was 4 in by 1 in by 25 in (10.16 cm by 2.54 cm by 63.5 cm), and the third size was 1 in by 1 in by 44 in (2.54 cm by 2.54 cm by 1.12 m). For the first and second channels, the shock tube diaphragm pressure ratio, P41, ranged from 6.0 to 20.0. The third channel was

DD FORM 1 JAN 73 1473 EDITION OF 1 NOV 65 IS OBSOLETE A

UNCLASSIFIED

SECURITY CLASSIFICATION OF THIS PAGE *(When Data Entered)*

Block 20.

used over a $P_{41}$ range of 8.0 to 20.0 and also to determine the presence of transverse waves due to an area reduction in the shock tube. The first channel, having the same cross-sectional area as the shock tube, exhibited pressures which approximated simple shock tube theory results. The second and third channels exhibited complex pressure changes which consistently peaked at the same time after the shock wave passed the pressure sensors, independent of $P_{41}$.

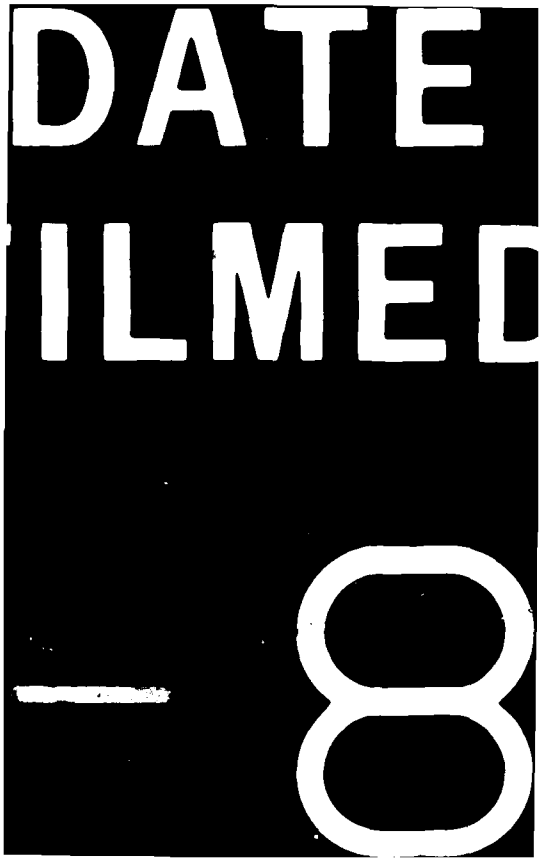
DATE
ILMED
8